

Slider Designs for Controlling Contamination: Simulation for Particles Moving in An Air Bearing

Shuyu Zhang and David B. Bogy

Computer Mechanics Laboratory

Department of Mechanical Engineering, University of California, Berkeley, CA 94720

Abstract

This paper presents a method for reducing the particle contamination on sliders. A model for simulating particle movement in an air bearing is developed and solved numerically. Through the simulation, the paths of particles moving in the air bearing are studied for various designs of sliders. It is found that some slider designs have good characteristics to make most of the particles entering the air bearing leave the slider from the sides instead of from the trailing edge, which is regarded as beneficial to reduce the particle contamination on the sliders.

Introduction

In magnetic hard drives, the storage density increases significantly with the reduction of the spacing between the recording head and the magnetic disk. The spacing, or “flying height” of the slider, is lower than 100 nm in most hard drives at present. At such a low flying height, the effects of particle contamination on drive reliability become very important, especially for removable cartridge-type hard drives.

Unfortunately, few studies relating to the particle contamination on sliders can be found in the open literature, although it has significant effects on drive reliability. Koka *et al* (1991) studied particle buildup on sliders and abrasive wear on disks resulting from particles accumulated in the leading edge tapers. Hiller *et al* (1991) presented the mechanism of particle contamination on sliders by studying the interaction of contaminant particles with a flying slider. They found that for the lubricated disk on which a slider flies, the contamination only concentrates on the tapers and trailing edge. The contamination on the trailing edge occurs in the form of whiskers. Some whiskers break off when the slider flies and are brought by the air flow into the tapers and deposit there again. It is observed that this indirect deposition is the main cause of contamination on the tapers.

Nomenclature

l = length of slider	R = gas constant
h_m = minimum film thickness	T_∞ = temperature of air
\mathbf{x}_p = particle position	T_w = temperature on wall of particle
\mathbf{v}_p = particle velocity	h = film thickness
\mathbf{v}_g = air flow velocity	p_a = ambient pressure
U, V = slider velocity	μ = air viscosity
\mathbf{X}_p = non-dimensional particle position; $\mathbf{X}_p = \mathbf{x}_p/l$	Λ_x, Λ_y = bearing number; $\Lambda_x = 6\mu U l / p_a h_m^2$, $\Lambda_y = 6\mu V l / p_a h_m^2$
\mathbf{V}_p = non-dimensional particle velocity; $\mathbf{V}_p = \mathbf{v}_p/U$	Q = flow factor
\mathbf{V}_g = non-dimensional air flow velocity; $\mathbf{V}_g = \mathbf{v}_g/U$	P = non-dimensional pressure; $P = p/p_a$
ρ_g, ρ_p = densities of air and particle	H = non-dimensional film thickness; $H = h/h_m$
m_p = particle mass	

Hiller *et al*'s experimental results provide us with very important information: if we can reduce the particle contamination on the trailing edge, then we can also reduce the contamination on tapers simultaneously. A strategy to realize this is to find ways to prevent particles from moving through the trailing edge, in other words, to make the particles move out of the air bearing surface from the two sides as early as possible.

In this paper, we use a numerical solution method to simulate particle movement in an air bearing. Through studying the paths of particles moving in the air bearing for various slider designs, we find some types that cause fewer particles to pass through the trailing edge.

Simulation model

Particle transport in a flow is a very complicated process because its motion is not only related to the undisturbed ambient flow, but also to the disturbance flow produced locally by its own motion. Maxey (1993) studied a single rigid spherical particle moving in an ambient flow and derived the motion equation. This is an integro-differential equation and its numerical solution is time-consuming. Actually, in many practical applications, the particle is very small and its disturbance to the ambient flow is negligible (Shimomizuki *et al* 1993; Liang *et al* 1993; Sommerfeld *et al* 1993; etc.). Therefore, as a first simplification in this paper, we deal with a single spherical particle moving in an air bearing and neglect its effects on the ambient flow.

The particle motion is treated by a Lagrangian approach with the equations:

d = particle diameter

D = non-dimensional particle diameter; $D = d/h_m$

kn = Knudsen number for particle; $kn = \lambda/d$

Kn = Knudsen number for film; $Kn = \lambda/h$

σ = squeeze number; $\sigma = 12\mu\omega l^2/p_0 h_m^2$

t = time variable

T = non-dimensional time; $T = \omega t$

X, Y = non-dimensional co-ordinates; $X = x/l, Y = y/l$

ΔT = integral step

$$\frac{d\mathbf{x}_p}{dt} = \mathbf{v}_p \quad (1-a)$$

$$m_p \frac{d\mathbf{v}_p}{dt} = \sum_i \mathbf{f}_i, \quad (1-b)$$

where m_p is the mass of the particle, \mathbf{x}_p is the position and \mathbf{v}_p the velocity vector of the particle in an air bearing, \mathbf{f}_i are forces acting on the particle. These forces include drag force, Saffman force (Saffman 1964), gravity force, Magnus force (Rubinow *et al* 1961), force caused by the pressure gradient and possibly others. Since the spacing of the air bearing is much smaller than the size of the slider, we can simplify the problem as a two dimensional one. Thus we can cancel the Saffman and gravity forces in equation (1-b). If we neglect the spin of the particle, the Magnus force can also be ignored. Note that the magnitudes of drag force and pressure related force are respectively $f_d \propto \rho_g v_g^2 d^2$ and $f_p \propto \frac{dp}{dn} d^3$. Since $p \sim \rho_g v_g^2$ and $d/l \ll 1$, we have $f_d \gg f_p$ and effects of pressure gradient can also be neglected. Thus, the only remaining force in (1-b) is drag force and equation (1-b) can be rewritten as:

$$m_p \frac{d\mathbf{v}_p}{dt} = \frac{\pi}{8} C_d \rho_g d^2 |\mathbf{v}_g - \mathbf{v}_p| (\mathbf{v}_g - \mathbf{v}_p), \quad (1-b')$$

where ρ_g is the density of the air, d is the diameter of the particle, \mathbf{v}_g is the velocity vector of air flow, and C_d is the drag coefficient, which is a function of \mathbf{v}_p and \mathbf{v}_g . Assuming the particle has uniform density, $m_p = \frac{\pi}{6} \rho_p d^3$. Substituting m_p together with non-dimensional variables and parameters into (1-a,b'), we obtain the following non-dimensional equations:

$$\frac{d\mathbf{X}_p}{dT} = R_l \mathbf{V}_p \quad (2-a)$$

$$\frac{d\mathbf{V}_p}{dT} = \frac{3}{4} \frac{R_d}{D} \frac{\rho_g}{\rho_p} C_d |\mathbf{V}_g - \mathbf{V}_p| (\mathbf{V}_g - \mathbf{V}_p) \quad (2-b)$$

where $\mathbf{X}_p = \mathbf{x}_p / l$, $\mathbf{V}_p = \mathbf{v}_p / U$, and $\mathbf{V}_g = \mathbf{v}_g / U$; $R_l = \frac{U}{\omega l}$, $R_d = \frac{U}{\omega h_m}$ and $D = d/h_m$ are non-dimensional numbers; ρ_p is the density of the particle.

To solve equations (2-a,b), an important step is the evaluation of the coefficient C_d . Since we are only interested in the particles with sizes that are the same or smaller than the spacing of the air bearing, which is usually smaller than the mean free path of air in commonly used hard drives at present, molecular slip occurs under such a situation which results in lower drag acting on the particles moving in the air bearing. Many researchers have worked in this field and presented their results for various conditions. An estimation of C_d for slip flow, which is believed to be useful for small Knudsen number, is obtained by applying a multiplication factor to the result of Stokes flow (Soo *et al* 1990):

$$C_d = \left(1 + 1.6 \times 10^{-5} kn\right) \frac{24}{R_e},$$

where R_e is the Reynolds number. For large Knudsen number, a more accurate approximation is one modifying the drag coefficient from molecular flow over a sphere (Liu *et al* 1965):

$$C_d = C_{dfm} [1 - B(S) / kn] \quad (3-a)$$

where the speed ratio $S = |\mathbf{v}_g - \mathbf{v}_p| / \sqrt{2RT_\infty}$, R is the gas constant, T_∞ is the temperature of the fluid away from the sphere; $B(S)$ is a function which ranges from 0.149 to 0.156 for S from 10^{-5} to 0.7, and 0.156 to 0.148 for S from 0.7 to 1. C_{dfm} is the free molecular drag of the sphere and is given by Schaaf *et al* (1961):

$$C_{dfm} = \frac{2}{S^2} \left[\frac{4S^4 + 4S^2 - 1}{4S} \operatorname{erf}(S) + \frac{e^{-S^2}}{\sqrt{\pi}} \left(S^2 + \frac{1}{2} \right) \right] + \frac{2}{3} \frac{\sqrt{\pi}}{S} \sqrt{\frac{T_w}{T_\infty}} \quad (3-b)$$

where T_w is the temperature on the wall of the sphere.

Note that (2-a,b) are four equations with four unknowns in component form and can be solved with given initial conditions and velocity field \mathbf{v}_g in the air bearing. Since we have assumed that the particle presence will not affect the flow in the air bearing, we can solve \mathbf{v}_g separately by using Reynolds equation in this case.

The classical Reynolds equation is actually a special case of combining continuum and momentum equations for solving the hydrodynamic lubrication problem. But due to the small spacing in the slider air bearing, the classical Reynolds equation which assumes no-slip and continuous flow is no longer valid, and several modifications were made based on slip boundary conditions and the Boltzmann equation (Burgdorfer 1959; Gans 1985; Fukui *et al* 1988). A generalized Reynolds equation was written as (Ruiz *et al* 1990):

$$\sigma \frac{\partial PH}{\partial T} = \frac{\partial}{\partial X} \left(QPH^3 \frac{\partial P}{\partial X} - \Lambda_x PH \right) + \frac{\partial}{\partial Y} \left(QPH^3 \frac{\partial P}{\partial Y} - \Lambda_y PH \right), \quad (4)$$

where Q is the flow factor and of different forms for the different types of modification models used,

$Q = 1,$	Continuum model
$Q = 1 + 6a \frac{Kn}{PH},$	1st order slip model
$Q = 1 + 6 \frac{Kn}{PH} + 6 \left(\frac{Kn}{PH} \right)^2,$	2nd order slip model
$Q = f \left(\frac{Kn}{PH} \right),$	Fukui-Kaneko model

where $a = \frac{2-\alpha}{\alpha}$ and α is the accommodation factor, $f \left(\frac{Kn}{PH} \right)$ is given by Fukui *et al* (1988; 1990). Note that the direct result of solving Reynolds equation is the pressure field P . After obtaining P , the velocity field \mathbf{v}_g in the air bearing can be calculated.

Numerical methods

The solution of the particle transport equation includes two parts: first, solve the Reynolds equation to obtain the pressure P , and then calculate the velocity field \mathbf{v}_g in the air bearing; second, solve the particle transport equation (2-a,b) with \mathbf{v}_g as a given condition.

To solve the Reynolds equation we use the finite difference method together with a multi-grid control volume method, which have been integrated into the CML air bearing design code, which

is a powerful and convenient software for slider designs. The detailed information about the finite difference and multi-grid control volume methods as well as the application of the CML air bearing design code can be found in related documents (Cha, *et al* 1995; Lu, *et al*, 1994; Lu, *et al* 1995; Shyy, *et al* 1993), and will not be presented in this paper.

For the solution of the particle transport equation, we use the classical Runge-Kutta method. Here we give a brief description of the application of this method in this problem. Actually, equations (2-a,b) can be generalized in component form as:

$$\frac{dZ_i}{dT} = fn_i(T, Z_1, Z_2, Z_3, Z_4), \quad Z_i(T_0) = Z_{i0}, \quad (i=1, \dots, 4) \quad (5)$$

where Z_i ($i=1, \dots, 4$) represent respectively X_p , Y_p , U_p , and V_p , the components of \mathbf{X}_p and \mathbf{V}_p ; the functions fn_i represent the corresponding RHS of equations (2-a,b), for instance, $Fn_3 = \frac{3}{4} \frac{R_d}{D} \frac{\rho_g}{\rho_p} C_d |\mathbf{V}_g - \mathbf{V}_p| (U_g - U_p)$ for the x -components of equation (2-b). With the particle

transport equations expressed as (5), the classical Runge-Kutta method can be written as:

$$Z_{i,n+1} = Z_{i,n} + \frac{\Delta T}{6} (k_{1,i} + 2k_{2,i} + 2k_{3,i} + k_{4,i}), \quad (i=1, \dots, 4) \quad (6-a)$$

$$k_{1,i} = fn_i(T_n, Z_{1,n}, \dots, Z_{4,n}), \quad (6-b)$$

$$k_{2,i} = fn_i\left(T_n + \frac{\Delta T}{2}, Z_{1,n} + \frac{\Delta T}{2} k_{1,1}, \dots, Z_{4,n} + \frac{\Delta T}{2} k_{1,4}\right), \quad (6-c)$$

$$k_{3,i} = f_{n_i} \left(T_n + \frac{\Delta T}{2}, Z_{1,n} + \frac{\Delta T}{2} k_{2,1}, \dots, Z_{4,n} + \frac{\Delta T}{2} k_{2,4} \right), \quad (6-d)$$

$$k_{4,i} = f_{n_i} (T_n + \Delta T, Z_{1,n} + \Delta T k_{3,1}, \dots, Z_{4,n} + \Delta T k_{3,4}), \quad (6-e)$$

where ΔT is the integral time step and n represents the n -th iteration.

Results and Discussions

Using the model and numerical method described in the previous sections, we simulate the particle movement in the air bearings for different sliders. For the convenience of comparison, 50% type sliders are chosen. In addition, the tapers for all simulated sliders have the same angle and length, 0.01 rad and 0.2 mm , and all sliders fly at the position 23 mm away from the center of the disks and while the disks rotate at 5400 rpm . To demonstrate the effects of this simulation method, the result for a simple tri-pad slider is shown in Fig. 1.

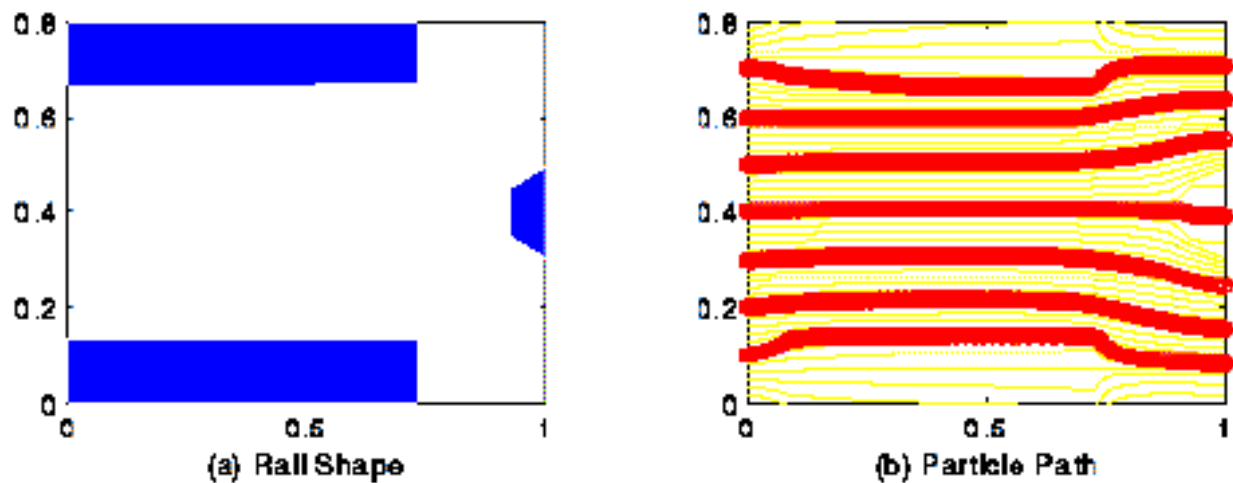


Fig.1 Particle movement simulation for a tri-pad slider

Figure (1a) shows the rail shapes of the slider. In (1b), the thin lines represent stream lines of the air flow and wide dark lines represent paths of particles moving in the air bearing. In this example, seven particles, all have the same diameter 30 nm and same initial velocity $0.7U$ in the x direction, are evenly spaced along the leading edge and simulated separately. The density of the particles is 2707 kg/m^3 (aluminum). The result shows that all particles move through the air

bearing and leave the slider from the trailing edge, which causes more chances for a particle to deposit at the trailing edge.

Table 1 gives some flying characteristics for this design. Note that the slider has a non-zero roll angle so the flow in the air bearing is not symmetric.

Table 1. Flying characteristics for the tri-pad slider

Rotation (<i>rpm</i>)	Skew (<i>rad</i>)	Pitch (μ <i>rad</i>)	Roll (μ <i>rad</i>)	Min FH(<i>nm</i>)
5400	0.0	230.2	8.9	33.4

Next we will introduce a special design selected from the simulation of various types of sliders, and compare it with a slider of “nutcracker” type. All the necessary parameters needed in the calculation are the same as those presented in the previous example. Fig. 2 shows the results for the two types of sliders.

In Fig. 2, design #1 is the nutcracker slider and #2 is the special slider design derived here with a concern for particle flow. The special characteristic of slider #2 is that it has two small rails at the leading corners. The main advantage of these two small rails is they construct two “channels” together with the central rail to produce the special flows in the air bearing to “lead” particles out of slider from the two sides. In addition, their existence also provides two tapers that are beneficial to the taking off of the slider and increases the flying stability of the slider. For the rail at the trailing edge, its sharp head provides a “secondary channel” which has a similar function as the “first channel”.

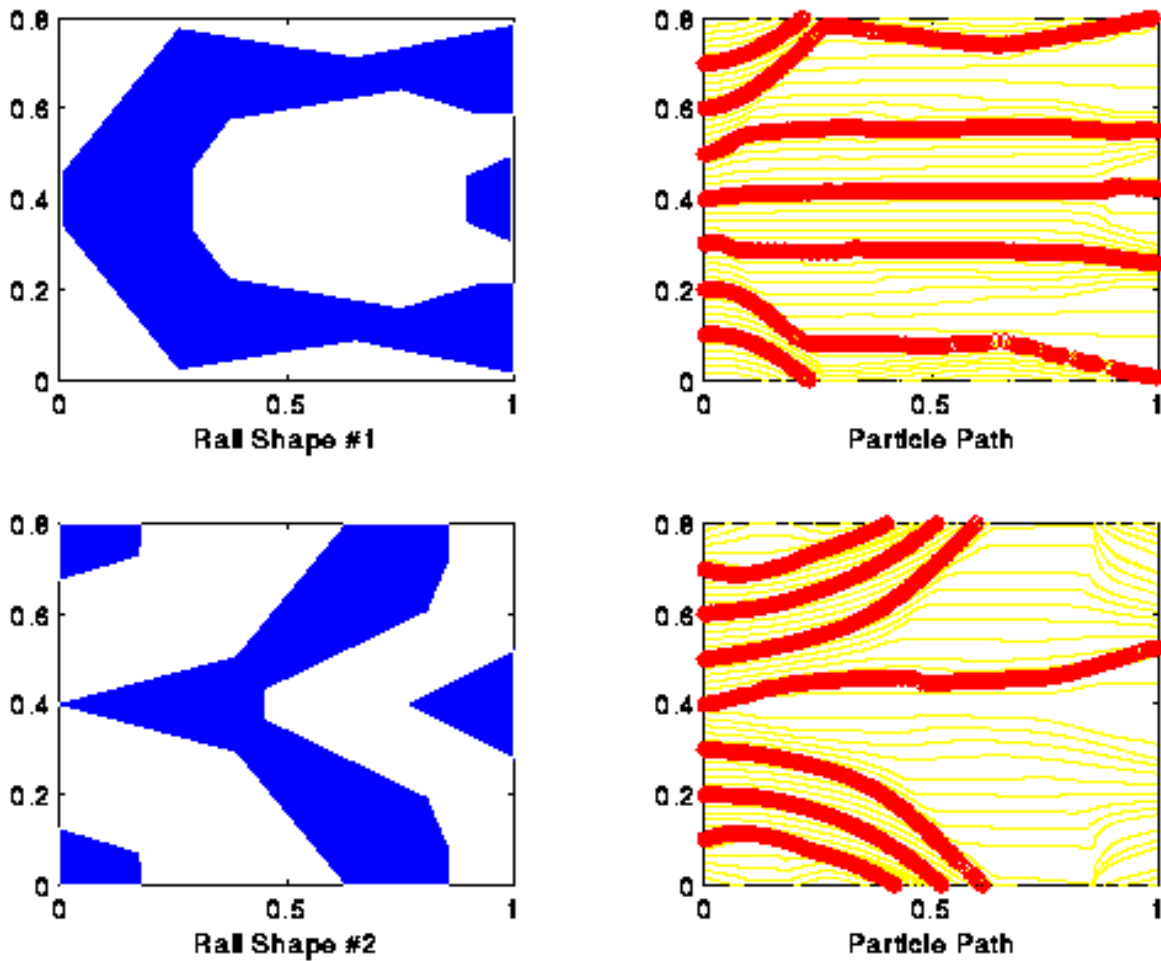


Fig. 2 Particle movement simulation: comparison of 2 sliders

Simulation results show that the particles follow the streamlines very well in both cases. An interesting aspect is that for design #2, some particles pass across the streamlines and move out of the slider faster than the streamlines. This is because the air flow slows down in these regions and makes the particle paths bend more sharply. Comparing the results for the two sliders, it is found that more particles pass through the air bearing and leave the slider from the trailing edge for slider #1 than for slider #2. From the view of reducing particle contamination, slider #2 is better than slider #1.

Table 2 provides some flying characteristics for the two designs. The minimum flying heights are respectively 35.1 *nm* for slider #1 and 31.3 *nm* for slider #2.

Table 2 Flying characteristics for 2 sliders

Designs	Rotation (<i>rpm</i>)	Skew (<i>rad</i>)	Pitch (μ <i>rad</i>)	Roll (μ <i>rad</i>)	Min FH (<i>nm</i>)
#1	5400	0.0	171.7	1.4	35.1
#2	5400	0.0	230.8	8.5	31.3

Summary

In this paper, a strategy for reducing particle contamination on a slider is determined, that is, to make the particles entering the air bearing leave the slider from the two sides as early as possible. A model for simulating particle movement in the air bearing is developed and solved numerically. Through the simulation, the paths of particles moving in the air bearing are studied for different types of sliders, and some good designs, which make most particles leave the sliders from the two sides, are selected. The results show that the particle transport simulation is a useful method for slider designs for controlling particle contamination.

References

- Burgdorfer, A., 1959, "The Influence of the Molecular Mean Free Path on the Performance of Hydrodynamic Gas Lubricated Bearings", *J. of Basic Engr.*, Vol. 81, p.94-100.
- Cha, E.T., Bogy, D.B., 1995, "A Numerical Scheme for Static and Dynamic Simulation of Subambient Pressure Shaped Rail Sliders", *J. of Tribology*, Vol. 117, p.36-46.
- Fukui, S., Kaneko, R., 1988, "Analysis of Ultra-thin Gas Film Lubrication Based on Linearized Boltzmann Equation: First report-Derivation of A Generalized Lubrication Equation Including Thermal Creep Flow", *J. of Tribology*, Vol. 110, p.253-261.
- Fukui, S., Kaneko, R., 1990, "A Database for Interpolation of Poiseuille Flow Rates for High Knudsen Number Lubrication Problems", *J. of Tribology*, Vol. 112, p.78-83.
- Gans, R., 1985, "Lubrication Theory at Arbitrary Knudsen Number", *J. of Tribology*, Vol. 107, p.431-433.
- Hiller, B., Singh, G.P., 1991, "Interaction of Contaminant Particles with the Particulate Slider/Disk Interface", *Adv. Info. Storage Syst.*, Vol. 2, p.173-180.
- Koka, R., Kumaran, A.R., 1991, "Visualization and Analysis of Particulate Buildup on the Leading Edge Tapers of Sliders", *Adv. Info. Storage Syst.*, Vol. 2, p.161-171.

Liang, Y., Shi, X., Xu, X., 1993, "Study on Turbulent Dispersion of Solid Particles in Plate Jet Near the Nozzle", (in Chinese), *J. of Engineering Thermophysics*, Vol. 14, No. 4, p.439-444.

Liu, V.C., Pang, S.C., Jew, H., 1965, "Sphere Drag in Flows of Almost-Free Molecules", *The Physics of Fluids*, Vol. 8, No. 5, p.788-796.

Lu, S., Bogy, D.B., 1994, "A Multi-Grid Control Volume Method for the Simulation of Arbitrarily Shaped Slider Air Bearings with Multiple Recess Levels", *CML report*, No. 94-016, UC Berkeley.

Lu, S., Bogy, D.B., 1995, "CML Air Bearing Design Program User's Manual", *CML report*, No. 95-003, UC Berkeley.

Maxey, M.R., 1993, "The Equation of Motion for A Small Rigid Sphere in A Nonuniform or Unsteady Flow", *Gas-Solid Flows*, Fed-Vol. 166, p.57-62.

Rubinow, S.I., Keller, J.B., 1961, "The Transverse Force on A Spinning Sphere Moving in A Viscous Fluid", *J. Fluid Mech.*, Vol. 11, part 3, p.447-459.

Ruiz, O.J., Bogy, D.B., 1990a, "A Numerical Simulation of the Head-Disk Assembly in Magnetic Hard Disk: 1. Component Model", *J. of Tribology*, Vol. 112, p. 593-602.

Saffman, P.G., 1965, "The Lift on A Small Sphere in A Slow Shear Flow", *J. Fluid Mech.*, Vol. 22, part 2, p. 385-400.

Shimomizuki, N., Adachi, T., et al, 1993, "Numerical Analysis of Particle Dynamics in A Bend of A Rectangular Duct by the Direct Simulation Monte Carlo Method", *Gas-Solid Flows*, Fed-Vol. 166, p.145-152.

Sommerfeld, M., Qiu, H., 1993, "Characterization of Particle-Laden, Confined Swirling Flows by Phase-Doppler Anemometry and Numerical Calculation", *Int. J. Multiphase Flow*, Vol. 19, No. 6, p. 1093-1127.

Schaaf, S.A., Chambre, P.L., 1961, "Flow of Rarefied Gases", *Princeton University Press*.

Shyy, W., Sun, C.S., 1993, "Development of A Pressure-correction/Staggered-grid Based Multi-grid Solver for Incompressible Recirculating Flows", *Computer and Fluids*, Vol.22, No. 1, p. 51-76.

Soo, S.L., et al, 1990, "Multiphase Fluid Dynamics", *Science Press*.